Military Technical College
Kobry El-Kobbah,
Cairo, Egypt.

18th International Conference on Applied Mechanics and Mechanical Engineering.

PARAMETRIC STUDY ON TAPER-ENDED TUBULAR SOLID PROPELLANT GRAINS

M. Y. Ahmed*

ABSTRACT

The design of the solid propellant grain is a decisive aspect of the solid propellant rocket motor performance. Tubular grain design is a favorable design since it produces a high neutral thrust profile. However, neutrality of tubular grains deteriorates as the aspect ratio of the grain deviates from an optimum value that is dependent on the web thickness. In some cases, the undesirable phenomenon of erosive grain burning may take place. One simple solution to restore neutrality is to add taper to the ends of the grain. Loss of motor filling comes as penalty for adding these tapered ends. The grain should thus be tailored to simultaneously satisfy both desired design objectives namely, neutrality and filling.

The present paper aims to address the dependence of these two design objectives on the design of a taper-ended tubular grain. The designs that are likely to yield erosive burning are also addressed. A parametric study is conducted involving the aspect ratio of the grain, its web thickness, and the taper angles on both ends.

KEYWORDS

Solid propellant rocket propulsion, Grain design, Neutrality, Filling coefficient, Erosive burning.

* Egyptian Armed Forces. Email: mahmoud.yehia@mtc.edu.eg

NOMENCLATURE

A_b Burning area, [m2]
A_b^* Burning area-to-grain outer cross section area, [m2]
D_{in} Inner diameter of propellant grain, [m]
D_{out} Outer diameter of propellant grain, [m]
K_F Volumetric filling coefficient, [-]
L Length of grain, [m]
L_{out} Outer length of the grain, [m]
L_{in} Length of inner cylindrical port of the grain, [m]
L^* Length- to- diameter ratio , [-]
y Instantaneous burnt distance, [m]
θ_h Head-end taper angle, [deg.]
θ_n Nozzle-end taper angle, [deg.]
τ Web thickness, [m]
τ^* Web thickness-to-grain outer radius ratio, [-]

INTRODUCTION

Compared with other types of rocket motors, solid propellant rocket motors (SPRM) have many advantages namely, they are simpler in design, easier in maintenance, safer in manipulation, have higher reliability, and longer storage life.

The solid propellant charge (the grain) once ignited, usually burns smoothly at a predetermined rate on all exposed surfaces of the grain. Thrust magnitude control is one of potential requirements addressed in some rocket applications. However, it is unmanageable to modify the thrust of SPRM once ignited. To solve this problem in SPRM, tailoring some parameters during the design phase would permit a reasonable predictable thrust history. The desired thrust history (profile) can be achieved via tuning the grain geometry, inhibiting some surfaces, and using different propellant compositions.

In almost all applications, neutral (single or dual) thrust profiles are desired since they yield the cruise flight preferred for proper flight control especially for guided rockets. A neural burning is attained using various grain geometries and inhibition styles. The simplest neutral burning grain configuration is the end-burning (cigarette) grain. This configuration also achieves the maximum filling (packing) of the motor cavity. However, the thrust level of the end-burning grains is low due to the small burning area.In contrast, a neutral burning with a high thrust level can be achieved using side (tubular) burning grains. This comes with the penalties of having a short operation time and a low motor filling. The filling of such design can be increased by reducing the inner and outer port areas. However, if the port areas are too small, the gas flow speed along the grain may reach values high enough to cause erosive burning; a phenomenon that produces an undesired progressive burning and yields a large amount of sliver. A compromise between the neutrality and filling can to a great extent be attained using internal burning (perforated) grains. If the perforation along the grain is properly designed, a nearly neutral burning can be achieved. The level of motor packing (filling) varies from one perforation design to another however, the main drawback of such grain design is the complexity of design and production in addition to the possibility of erosive burning in some designs.

One simple design that can achieve a neutral burning as well as high motor filling is the end-tubular burning grain. This grain is inhibited from the outer peripheral surface only and is allowed to burn from all other surfaces. If the dimensions of the grain are properly set, a neutral burning can be achieved. Neutrality may deteriorate for longer grains of this type. Adding tapering to grain ends was found to restore neutrality however, loss in filling emerged as a penalty [4].

Neutrality and filling of these taper-ended tubular grains are believed to be dependent on the their configuration. The present work is intended to conduct a parametric study on the dependence of neutrality and filling of such grains on their design. Mathematical expressions for these two merits are derived in terms of the grain design parameters and are applied for a large number of distinct designs that are generated using a space-filling sampling approach. The present work can be viewed as an extension for the work of Noaman et al. [4]. In that work, neutrality and filling of the same grain configuration were examined only for web thickness of 0.4 and three values of taper angles (equal in both sides). Here, the web thickness is varied and the entire design space is expanded. In addition, along with neutrality and filling, erosive burning that may take place for some designs is taken into consideration. This likelihood is addressed for specific ballistic environment. The maximum combustion gas flow velocity along the grain is taken as a measure of erosive burning occurrence. The remainder of the paper is organized as follows. The sampling methodology is presented next along with the full derivations for neutrality, filling, and erosive burning measure. The following section presents and discusses the main findings of the study. The paper finalizes with main conclusions of the study.

CASE STUDY AND METHODOLOGY

Case Study and Sampling Approach

The geometry of the taper-ended tubular grain in concern is shown in Fig. 1. For a given rocket motor caliber, $\mathrm{D_{out}}$, the grain geometry can be fully represented by four independent geometrical parameters namely, the web thickness, the grain length, and the taper angles on both sides of the grain. For a more generic representation, the web thickness and grain length are referred to the grain caliber, $\mathrm{D_{out}}$, as follows:
The relative web thickness:

$$\tau^* = \frac{2\tau}{\mathrm{D_{out}}} = 2 * \frac{0.5 * (\mathrm{D_{out}} - \mathrm{D_{in}})}{\mathrm{D_{out}}} = 1 - \frac{\mathrm{D_{in}}}{\mathrm{D_{out}}}$$

The mean grain slenderness ratio:

$$\mathrm{L^*} = \frac{\mathrm{L}}{\mathrm{D_{out}}} = 0.5 * \frac{(\mathrm{L_{out}} + \mathrm{L_{in}})}{\mathrm{D_{out}}}$$

The head-end taper angle: θ_h
The nozzle-end taper angle: θ_n

By independently varying these four parameters within some upper and lower respective bounds, various distinct designs can be generated. In this work, the lower and upper bounds of variation for these four parameters are listed in Table 1.

Samples are selected from the developed four-dimensional design space using the full-factorial sampling technique. With 9, 10, 9 and 9 divisions for τ^*, L^*, θ_h, and θ_n, respectively, a total of 7290 samples (each representing a distinct grain design) is generated. For each design, the neutrality, filling, and erosive burning criterion is calculated using the formula derived below.

Neutrality Coefficient

Neutrality of burning is express how the produced thrust maintains a constant value over the motor operation time. For solid propellant grains, neutrality is achieved if the area of burning surface maintains a nearly constant value over the entire operation time. There are many measures of neutrality; here, the ratio between the maximum and average burning surface areas of the grain is taken as a measure of neutrality. Following this definition, neutrality coefficient is generally greater than 1 and the best neutrality value is 1 which indicates that the maximum burning surface area is equal to the average burning surface area. In what follows, this expression for neutrality is derived under the following two assumptions:

During the burning process, the burning surface moves parallel to the initial surface, Fig. 2. At any instant of time, the dashed line marks the instantaneous burning surface.

The length of the inner cylindrical port, L_{in}, remains greater than zero over the entire motor operation time. Hence, an axial section along the burning surface will retain a trapezoidal rather than a triangular shape over the entire burning time. This implies that the grain dimensions are such that it is consumed axially from both sides before the inner cylindrical surface reaches the outer one. Out of the 7290 samples generated in the design space presented above, 551 samples violate this condition and are eliminated from the samples.

Following the above assumptions, for a given burnt distance, y, the burning area can be expressed as:

$$A_b = \pi(D_{in} + 2y)\left[L_{in} - y\left(\tan\left(\frac{\theta_h}{2}\right) + \tan\left(\frac{\theta_n}{2}\right)\right)\right] + \frac{\pi}{2}(D_{out} + D_{in} + 2y)\left[\left(\frac{\tau - y}{\sin(\theta_h)}\right) + \left(\frac{\tau - y}{\sin(\theta_n)}\right)\right] \quad (1)$$

Substituting in the above equation for the following geometric relations:

$$L_{in} = L - \frac{H_1}{2} - \frac{H_2}{2} \qquad \tan\left(\frac{\theta}{2}\right) = \frac{1}{\sin(\theta)} - \frac{1}{\tan(\theta)}$$

$$H_1 = \frac{\tau}{\tan(\theta_h)} \qquad H_2 = \frac{\tau}{\tan(\theta_n)} \qquad D_{in} = D_{out} - 2\tau$$

Equation (1) will have the form:

$$\begin{aligned} A_b = \pi \Bigg[& L(D-2\tau) - \frac{2yD}{\sin(\theta_h)} - \frac{2yD}{\sin(\theta_n)} + \frac{3y\tau}{\sin(\theta_h)} + \frac{3y\tau}{\sin(\theta_n)} + \frac{yD}{\tan(\theta_h)} + \frac{yD}{\tan(\theta_n)} \\ & - \frac{3y\tau}{\tan(\theta_h)} - \frac{3y\tau}{\tan(\theta_n)} + 2yL - \frac{3y^2}{\sin(\theta_h)} - \frac{3y^2}{\sin(\theta_n)} + \frac{2y^2}{\tan(\theta_h)} \\ & + \frac{2y^2}{\tan(\theta_n)} - \frac{\tau D}{2\tan(\theta_h)} - \frac{\tau D}{2\tan(\theta_n)} + \frac{\tau^2}{\tan(\theta_h)} + \frac{\tau^2}{\tan(\theta_n)} + \frac{\tau D}{\sin(\theta_h)} \\ & - \frac{\tau^2}{\sin(\theta_h)} - \frac{\tau^2}{\sin(\theta_n)} + \frac{\tau y}{\sin(\theta_h)} + \frac{\tau y}{\sin(\theta_n)} \Bigg] \end{aligned} \quad (2)$$

Now, introducing the following dimensionless terms:

$$A_b^* = \frac{4A_b}{\pi D_{out}^{\ 2}} \qquad \tau^* = \frac{2\tau}{D_{out}} \qquad y^* = \frac{y}{\tau} \qquad L^* = \frac{L}{D_{out}}$$

Eventually, Eqn. (2) will have the form:

$$A_b^* = a + by^* + cy^{*2}$$

where:

$$a = 4L^*(1-\tau^*) + \left(\frac{1}{\tan(\theta_h)} + \frac{1}{\tan(\theta_n)}\right)\left(-\tau^* + \tau^{*2}\right) + \left(\frac{1}{\sin(\theta_h)} + \frac{1}{\sin(\theta_n)}\right)\left(2\tau^* - \tau^{*2}\right)$$

$$b = 4\left(\frac{1}{\sin(\theta_h)} + \frac{1}{\sin(\theta_n)}\right)\left(-\tau^* + \tau^{*2}\right) + \left(\frac{1}{\tan(\theta_h)} + \frac{1}{\tan(\theta_n)}\right)\left(2\tau^* - 3\tau^{*2}\right) + 4\tau^* L^* \quad (3)$$

$$c = -\frac{3\tau^{*2}}{\sin(\theta_h)} - \frac{3\tau^{*2}}{\sin(\theta_n)} + \frac{2\tau^{*2}}{\tan(\theta_h)} + \frac{2\tau^{*2}}{\tan(\theta_n)}$$

Finally, neutrality is defined as the ratio of the maximum to the average burning surfaces encountered during the burning duration, i.e.,:

$$N = (A_b^*)_{max}/(A_b^*)_{average} \quad (4)$$

where:

$$(A_b^*)_{max} = a - \frac{b^2}{4c} \qquad (A_b^*)_{average} = a + \frac{b}{2} + \frac{c}{3}$$

Filling Coefficient

The filling reflects the level of packing of propellant inside the rocket motor. Here, the coefficient of volumetric filling is implemented to describe the level of filling. It is defined as the ratio of the grain volume to the available empty motor volume. These two volumes are expressed, respectively, as:

$$V_P = \frac{\pi}{4}(D_{out}^2 - D_{in}^2)L = \frac{\pi}{4}[D_{out}^2 - (D_{out} - 2\tau)^2]L = \frac{\pi}{4}L(4D_{out}\tau - 4\tau^2)$$

$$V_m = \frac{\pi}{4} L_{out} {D_{out}}^2 = \frac{\pi}{4}\left(L + \frac{H_1}{2} + \frac{H_2}{2}\right) {D_{out}}^2 = \frac{\pi}{4}\left[L + \frac{\tau}{2\,tan(\theta_h)} + \frac{\tau}{2tan(\theta_n)}\right] {D_{out}}^2$$

Hence, the volumetric filling coefficient is expressed as:

$$K_F = \frac{V_P}{V_m} = \left[\frac{(4\tau D_{out} - 4\tau^2)/{D_{out}}^2}{1 + \left(\frac{\tau}{2L}\right)\left(\frac{1}{tan(\theta_h)} + \frac{1}{tan(\theta_n)}\right)}\right] = \left[\frac{2\tau^* - {\tau^*}^2}{1 + \left(\frac{\tau^*}{4L^*}\right)\left(\frac{1}{tan(\theta_h)} + \frac{1}{tan(\theta_n)}\right)}\right] \quad (5)$$

The volumetric filling coefficient has a theoretical maximum value of 1; a value of this coefficient closer to 1 is better.

Erosive burning

Erosive burning is defined as the augmentation of grain burning rate due to excessive gas flow speed along the grain port [1, 2]. Clearly, erosive burning is undesirable since it yields unpredictable thrust profiles as well as considerable amount of sliver. As a rule of thumb, if the velocity of combustion gases through the port reaches 200 m/s, erosive burning occurs. For the grain configuration considered in this study, erosive burning can take place in some designs and it is desired to determine these designs. To do so, the maximum combustion gas velocity is estimated. It is the gas velocity at the nozzle-end of inner cylindrical port of the grain immediately at the onset of combustion calculated as:

$$A_P = \frac{\pi}{4} {D_{in}}^2 = \frac{\pi}{4}(D_{out} - 2\tau)^2$$

The gases flowing through this area are generated as a result of combustion of all upstream burning surfaces calculated as:

$$A_g = \pi \mathrm{D}_{in} L_{in} + \frac{\pi}{2}(D_{in} + D_{out})\left[\frac{\tau}{sin(\theta_h)}\right]$$
$$= \pi(D_{out} - 2\tau)\left(L - \frac{\tau}{tan(\theta_h)} - \frac{\tau}{tan(\theta_n)}\right) + \frac{\pi}{2}(2D_{out} - 2\tau)\left[\frac{\tau}{sin(\theta_h)}\right]$$

Dividing A_g by A_P,

$$\frac{A_g}{A_P} = \frac{4\left(L - \frac{1}{2}\left(\frac{\tau}{tan(\theta_h)} + \frac{\tau}{tan(\theta_n)}\right)\right)}{D_{out} - 2\tau} + \left(1 + \frac{D_{out}}{D_{out} - 2\tau}\right)\left(\frac{\tau}{(D_{out} - 2)sin(\theta_h)}\right)$$

Dividing both nominator and denominator by $\frac{\pi}{4}{D_{out}}^2$,

$$\frac{A_g}{A_P} = \frac{4}{(1 - \tau^*)}\left[L^* - \frac{1}{2}\left(\frac{\tau^*}{tan(\theta_h)} + \frac{\tau^*}{tan(\theta_n)}\right)\right] + \left(1 + \frac{1}{1 - \tau^*}\right)\left[\frac{\tau^*}{(1 - \tau^*)sin(\theta_h)}\right] \quad (6)$$

Based on continuity principle, the mass flow rate of combustion gases through any given port is equal to their rate of generation from all upstream surfaces [3]. Hence:

$$V_g A_P \rho_g = A_g \rho_{sp} r \qquad \text{or:} \qquad V_g = \frac{A_g}{A_P}\frac{\rho_{sp}}{\rho_g} r$$

where A_g/A_P is defined in Eqn. (6) and ρ_{sp} and ρ_g are the densities of the solid propellant and combustion gas products, respectively. r is the rate of burning of the propellant that is dependent on the combustion pressure according to the burning law relation [1, 2]. For any design, if V_g exceeds the value of $200\ m/s$, erosive burning takes place causing the undesirable excessive regression pattern. Clearly, estimating the erosive burning requires specifying the ballistic properties of the used propellant. Here, the properties of a typical double-base propellant listed in the table below are used.

RESULTS AND DISCUSSIONS

Samples Distribution in the Objective Space

Figure 3a below shows the distribution of all samples in the two-dimensional objective space with neutrality and filling as the space coordinates. Here, only the 6738 samples that obey the constraints for inner cylinder length are plotted. The solid markers refer to the samples that encounter erosive burning based on the ballistic conditions proposed above. The hollow markers refer to the samples that are expected to experience no erosive burning. A zoom-in at the Pareto front of all samples is illustrated in Fig. 9b whereas Fig. 9c shows the Pareto front of all samples with no erosive burning.

It is clear that the two objectives namely, maximum filling and minimum neutrality are competing. A single sample that possesses both maximum filling and minimum (best) neutrality does not exist. As the filling coefficient values of the samples approach the maximum value of 1, the corresponding neutrality coefficient values shift further higher than the minimum value of 1. In addition, samples that have the upper values of filling; samples with filling higher than 0.96 always encounter erosive burning.

Variation of Filling Coefficient with the Design Parameters

The figure below illustrates samples of the variation of filling coefficient with the grain design parameters. Examining the above figures reveals the following. Grain filling coefficient increases with the increase in web thickness for all grain lengths. For a given web thickness, as the taper angles on both ends increases, the filling increases; perfectly cylindrical grains (with no taper ends) yield the maximum filling. The effect of taper angles is insignificant in grains with small web thickness and becomes more pronounced as the web thickness increases. The impact of grain length on filling coefficient may not be clear in the above figure. This role is illustrated more clearly in Fig. 5 below.

As inferred from the above figure, for grains with small web thickness, as the grain length increases, the filling improves however, this role is more pronounced at small taper angles. For perfectly cylindrical grains (with small web thickness), the grain length has an insignificant effect on the filling coefficient. In contrast, for grains with large web thickness and small taper angles, shorter grains yield higher filling than

longer ones. On the other hand, a higher filling can be achieved with large web thickness and high taper angles if longer grains are used.

Variation of Neutrality with the Design Parameters

The figure below illustrates samples of the variation of neutrality coefficient with the design parameters.

Figure 6 shows that neutrality increases as the web thickness increases. For short grains, the best (minimum) neutrality is achieved at high taper angles and becomes higher (worse) as the taper angles decrease. For longer grains, the behavior of neutrality changes. The best (minimum) neutrality is associated with small taper angles. It then deteriorates (increases) as the taper angles increase (up to about 60^o) and slightly improves as the taper angles increase further. The dependence of neutrality coefficient can be further understood from Fig. 7 below.

Design Parameters of Extreme and Compromised Grain Designs

Finally, the design parameters of grains that show the extreme (maximum and minimum) values of both merits namely, filling and neutrality coefficients are presented. Table 3 below lists the design parameters of these extreme merit values. Since the length is the key design factor for solid propellant motors, the grain length is takes as the primary entry in the table below. The corresponding value of the other merit is also shown.

For all grain lengths, cylindrical designs yield the maximum filling coefficient. For short and medium-length grains, the maximum possible web thickness is ($\tau^* = 0.8$, for the used type of propellant). Grains with web thickness ($\tau^* = 0.9$) are not shown in the table since they all experience an erosive burning regardless to their length. As the grain length increases, erosive burning takes place in grains with ($\tau^* = 0.8$) and the maximum allowable grain thickness for such long grains is ($\tau^* = 0.7$) resulting in a drop in the filling coefficient. Grains with minimum filling are indeed the ones with minimum web thickness and taper angles of both ends regardless to the grain length. The filling coefficient increases slightly as the grain length increases. The values of neutrality corresponding to maximum and minimum filling are neither the “desired” minimum nor the maximum ones, respectively. In contrast, no specific criteria can be identified for designs with the best (minimum) neutrality. However, the best neutrality can be related to small taper angles on both ends resulting in low filling. Of all samples tested, the grain lengths of 2, 4, and 4.5 times the outer diameter yield the best neutrality. Grains as short as half the caliber yield the worst neutrality compared with longer grains.

As inferred from the Table as well as from Fig. 3, no single grain can achieve both maximum filling and minimum neutrality. If a compromise design is sought, a new formula aggregating both merits is proposed. The proposed compromise merit function is defined here as the ratio between neutrality and filling, N/K_F; a grain design with a minimum value of N/K_F is considered better in both objectives and vice versa. The grain designs with extreme values of the proposed formula are listed in Table 4 with grain length as the main entries. The corresponding values for both N and K_F are listed. Generally, thick grains with right end(s) yield the minimum (best) values of the proposed merit function. In contrast, thin grains with highly-tapered

ends yield the maximum (worst) merit function values. Of all grain designs tested, a 2-caliber long grain would yield the best merit function value. It should be noted that if a definition for the merit function other than the one proposed here, N/K_F, is to be adopted, the designs shown in Table 4 are expected to vary.

CONCLUSIONS

The ballistic behavior of internal-end burning solid propellant grains is inspected in the present work. Neutrality, filling and likelihood of erosive burning of such grain design have been collectively investigated through a parametric study involving four design parameters. it has been found that, erosive burning can take place for thick and long grains. Neutrality and filling of normally (non-erosive) burning grains are found competing. The impact of the design parameters on the performance merits is explained and visualized. Recommendations for compromise grain designs are proposed.

REFERENCES

[1] Sutton, G. P., "Rocket Propulsion element," Seventh edition, John Wiley,1992.
[2] Barrere, M., Jaumotte, A., De veubeke, B. F. and Vandenkerckhove, J.," Rocket Propulsion," Elsevier publishing company, 1960.
[3] Noaman, H. R., Ahmed, M. Y., Abdalla, H. M. and Al-Sanabawy, M. A., “Neutrality of Taper-Ended Tubular Grains,” 15th International Conference on Aerospace Sciences and Aviation Technology, ASAT – 15, May 28 - 30, 2013.

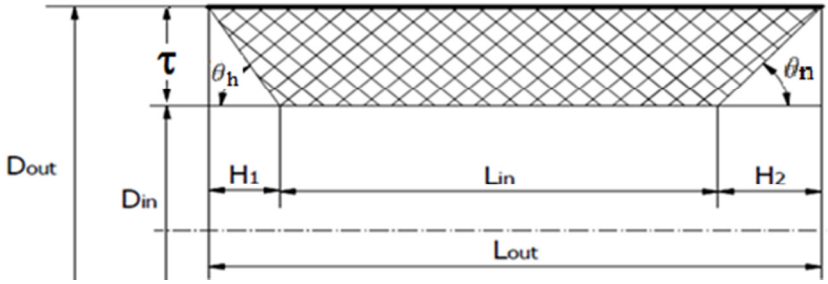

Fig. 1. Configuration and design parameters of taper-ended tubular grains.

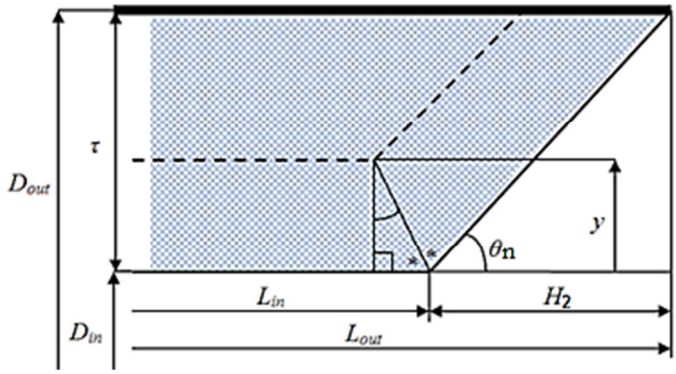

Fig. 2. Regression style of the grain.

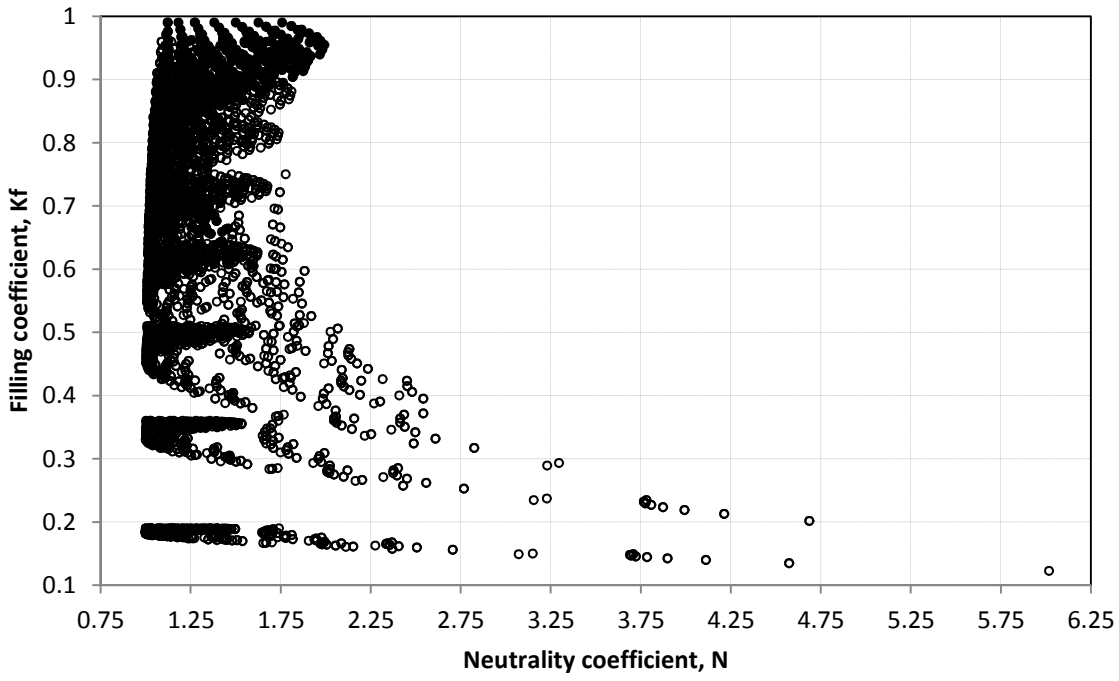

(a)

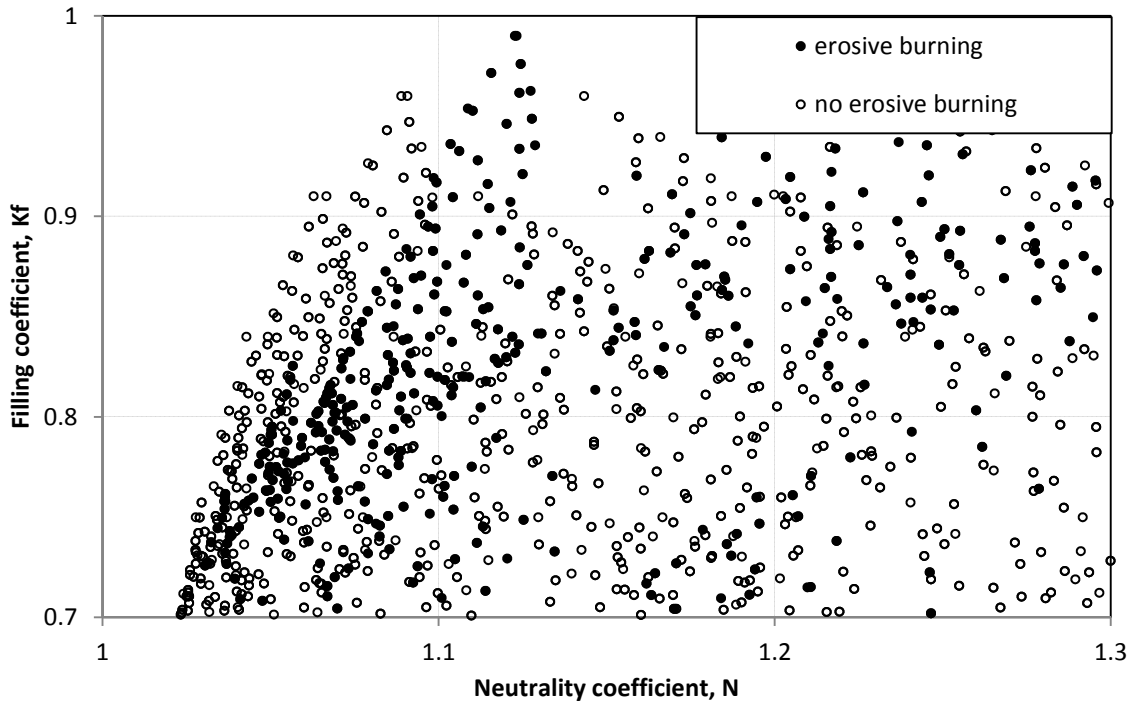

(b)

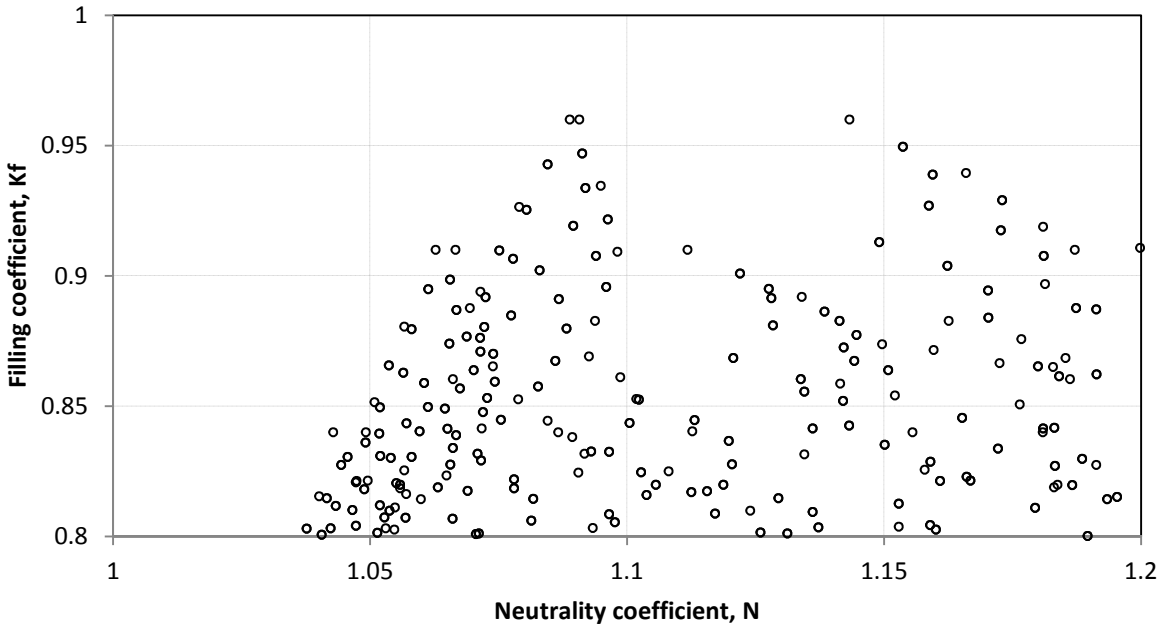

(c)

Fig. 3. Distribution of samples in the objective space.

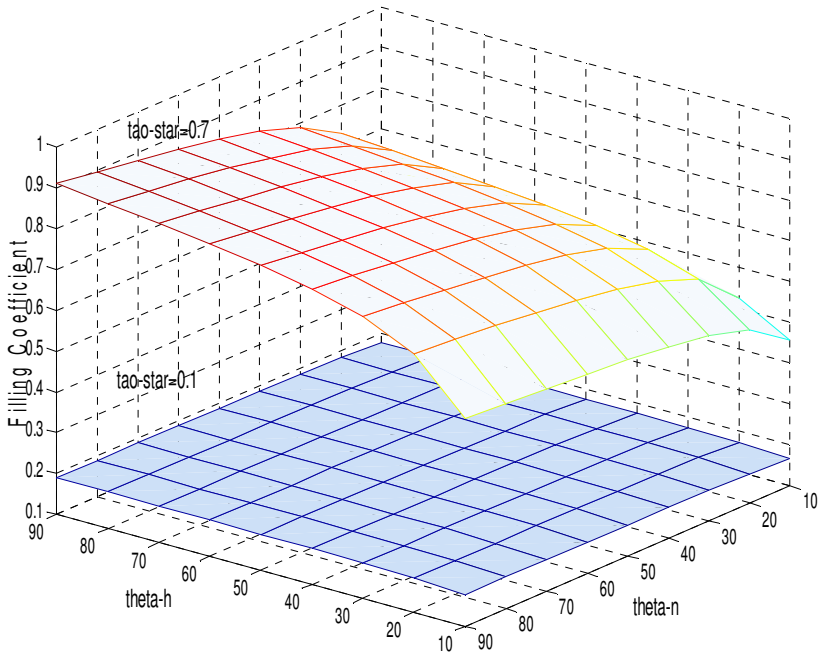

(a) $L^* = 2$

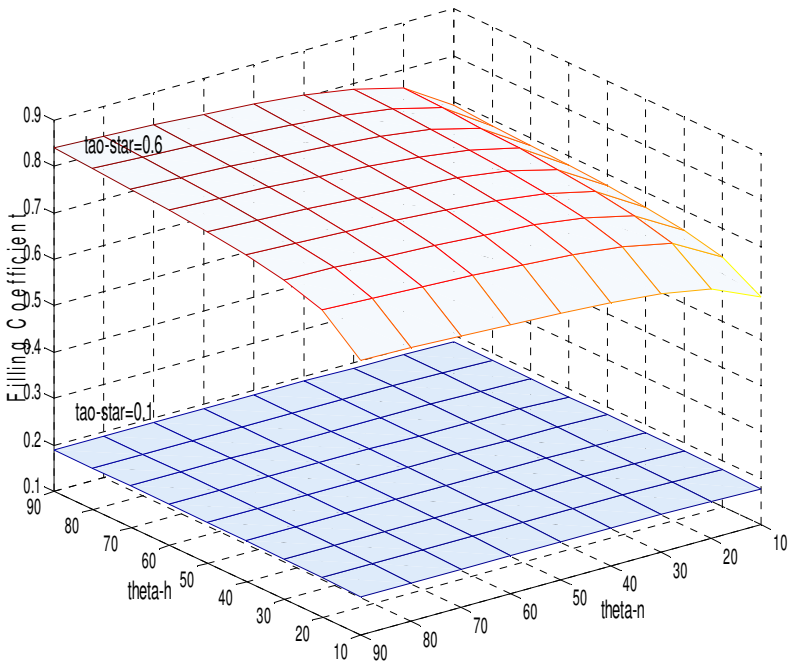

(b) $L^* = 4$

Fig. 4. Variation of filling coefficient with design parameters for different L^*

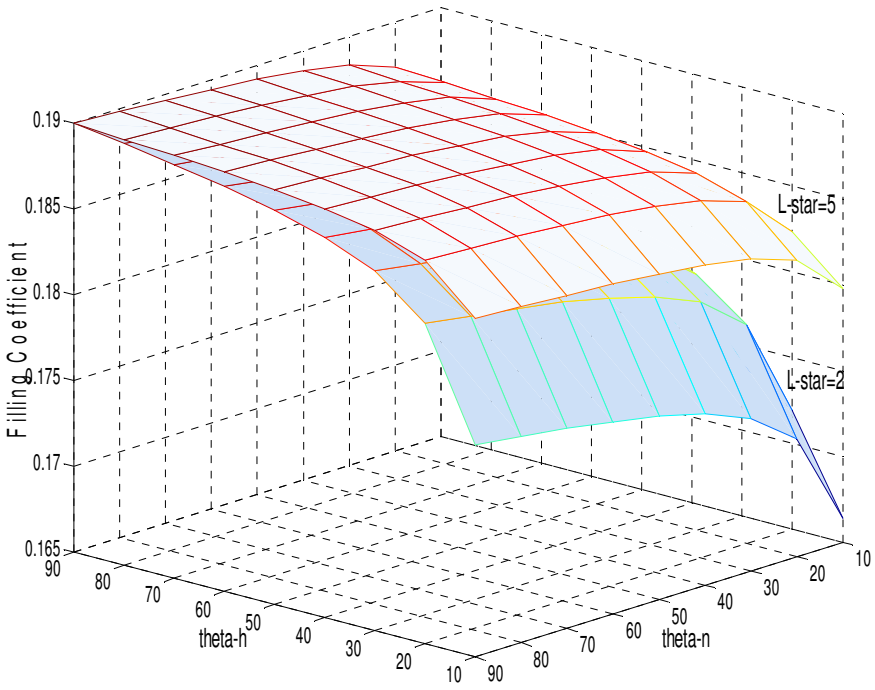

(a) $\tau^* = 0.1$

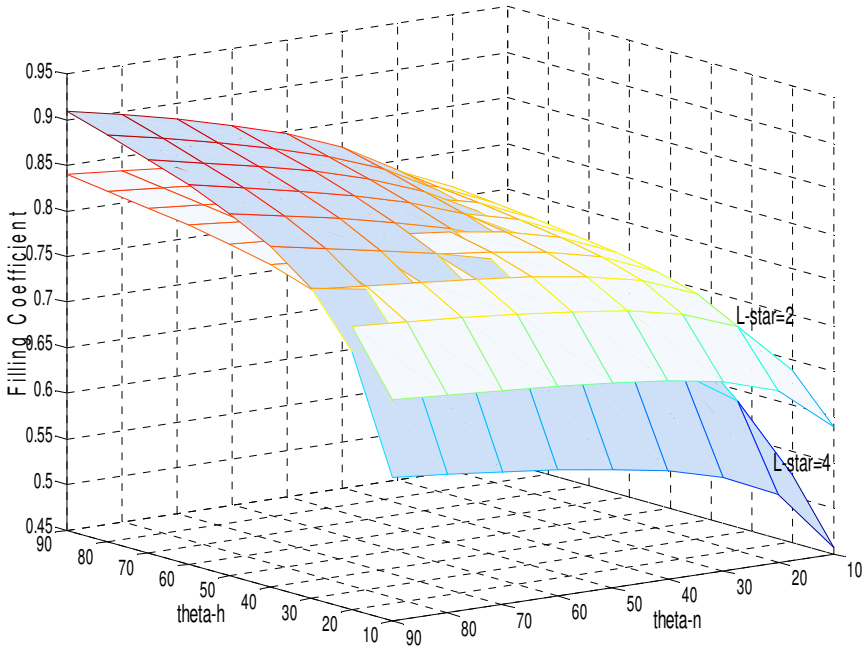

(b) $\tau^* = 0.6$

Fig. 5. Variation of filling coefficient with design parameters for different τ^*.

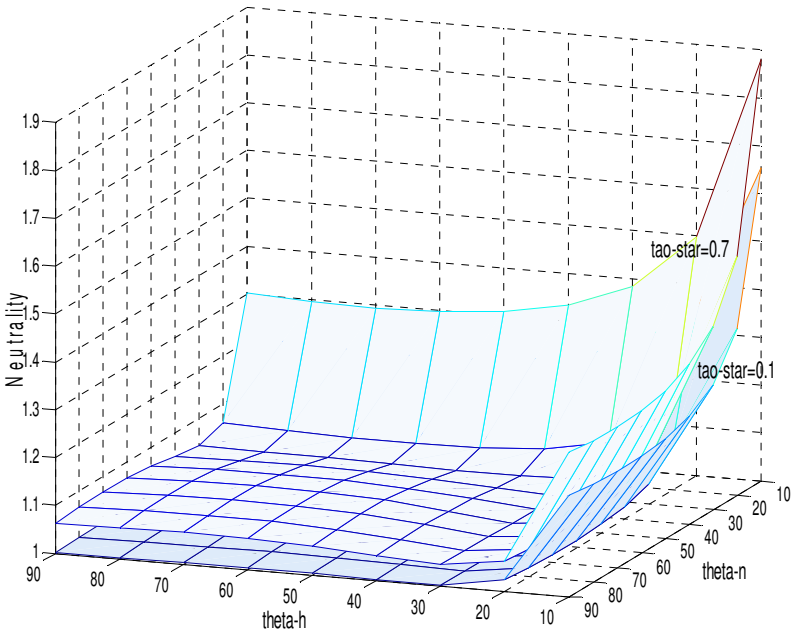

Fig. 6. Variation of neutrality coefficient with design parameters for $L^* = 2$.

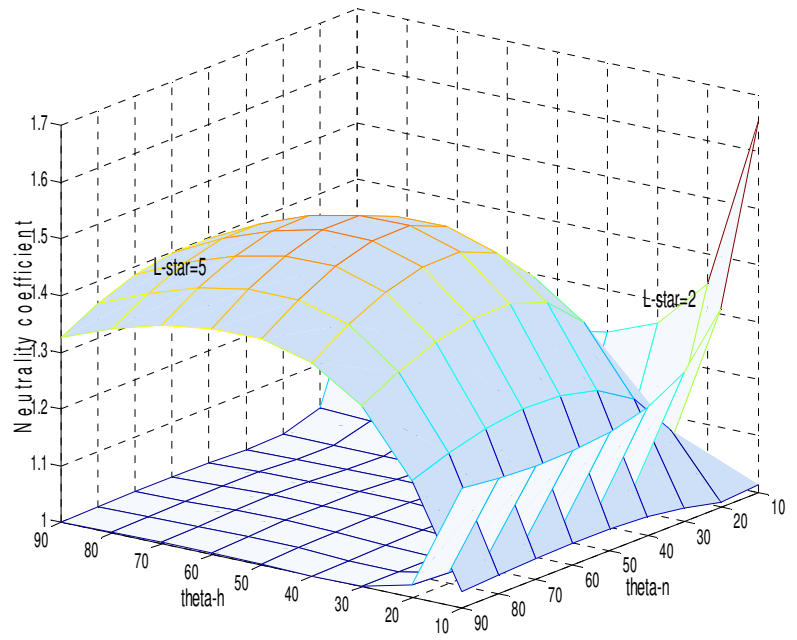

Fig. 7. Variation of neutrality coefficient with design parameters for $\tau^* = 0.1$.

Table 1. Lower and upper bounds of grain design parameters.

Design parameter	Lower bound	Upper bound
Relative web thickness, τ^*	0.1	0.9
Mean grain slenderness ratio, L^*	0.5	5
Head-end taper angle, θ_h	10^o	90^o
Nozzle-end taper angle, θ_n	10^o	90^o

Table 2. Ballistic properties of the used propellant for erosive burning calculations.

Ballistic property	Value
Combustion pressure, P_c [bar]	70
Burning law	$r = 0.713 \times 10^{-5} P^{0.569}$
Burning rate at P_c, $[m/s]$	0.008
Propellant density, ρ_{sp}, $[Kg/m^3]$	1563
Combustion gas density, ρ_g, $[Kg/m^3]$	6.05

Table 3. Grain designs with extreme neutrality and filling coefficients.

L^*	Best (minimum) neutrality					Worst (maximum) Neutrality				
	N	τ^*	θ_h	θ_n	K_F	N	τ^*	θ_{hh}	θ_n	K_F
0.5	1.6473	0.1	70	70	0.18	6.0174	0.1	10	10	0.12
1	1.1130	0.2	70	70	0.348	3.2303	0.3	10	10	0.29
1.5	1.0069	0.1	60	60	0.186	2.3173	0.5	10	10	0.42
2	1.0005	0.1	50	30	0.184	1.8398	0.6	10	10	0.51
2.5	1.0005	0.1	40	20	0.183	1.5642	0.7	10	10	0.58
3	1.0009	0.1	20	20	0.182	1.3344	0.6	10	10	1.33
3.5	1.0032	0.1	60	10	0.182	1.4271	0.8	60	70	0.92
4	1.0005	0.1	30	10	0.182	1.5214	0.7	60	60	0.87
4.5	1.0005	0.1	20	10	0.182	1.6637	0.7	60	60	0.88
5	1.0069	0.1	20	10	0.183	1.8108	0.7	60	60	0.88

L^*	Best (maximum) Filling					Worst (minimum) Filling				
	K_F	τ^*	θ_h	θ_n	N	K_F	τ^*	θ_{hh}	θ_n	N
0.5	0.75	0.5	90	90	1.78	0.1224	0.1	10	10	6.017
1	0.96	0.8	90	90	1.23	0.1488	0.1	10	10	3.072
1.5	0.96	0.8	90	90	1.09	0.1603	0.1	10	10	2.113
2	0.96	0.8	90	90	1.09	0.1668	0.1	10	10	1.65
2.5	0.96	0.8	90	90	1.14	0.1710	0.1	10	10	1.39
3	0.96	0.8	90	90	1.26	0.1739	0.1	10	10	1.24
3.5	0.96	0.8	90	90	1.32	0.1760	0.1	10	10	1.14
4	0.91	0.7	90	90	1.38	0.1776	0.1	10	10	1.076
4.5	0.91	0.7	90	90	1.48	0.1789	0.1	10	10	1.036
5	0.91	0.7	90	90	1.6	0.1800	0.1	10	10	1.013

Table 4. Grain designs with extreme compromise merit function.

L^*	Best (minimum) merit function; N/K_F					
	N/K_F	τ^*	θ_h	θ_n	N	K_F
0.5	2.3704	0.5	90	90	1.7778	0.75
1	1.2847	0.8	90	90	1.2333	0.96
1.5	1.1362	0.8	90	90	1.0907	0.96
2	1.1343	0.8	90	90	1.0889	0.96
2.5	1.1910	0.8	90	90	1.1433	0.96
3	1.2770	0.8	90	90	1.2259	0.96
3.5	1.3798	0.8	90	90	1.3246	0.96
4	1.3610	0.7	10	90	1.0365	0.762
4.5	1.3568	0.7	10	90	1.0517	0.775
5	1.3741	0.7	10	90	1.0805	0.786

L^*	Worst (maximum) merit function; N/K_F					
	N/K_F	τ^*	θ_h	θ_n	N	K_F
0.5	49.143	0.1	10	10	6.0174	0.1224
1	20.6487	0.1	10	10	3.0717	0.1488
1.5	13.1785	0.1	10	10	2.1128	0.1603
2	9.9165	0.1	10	10	1.6543	0.1668
2.5	8.16739	0.1	10	10	1.3965	0.1710
3	7.1271	0.1	10	10	1.2393	0.1739
3.5	6.4743	0.1	10	10	1.1395	0.1760
4	6.9033	0.1	50	50	1.2983	0.1881
4.5	7.4138	0.1	50	50	1.3958	0.1883
5	7.9461	0.1	50	50	1.4974	0.1884